

RESEARCH ARTICLE

View Article Online
View Journal | View Issue



Cite this: *Mater. Chem. Front.*,
2018, 2, 76

Non-covalent molecular tweezer/guest complexation with Pt(II)···Pt(II) metal–metal interactions: toward intelligent photocatalytic materials†

Zijian Li, Yifei Han, Zongchun Gao, Tengfei Fu and Feng Wang *

A new organoplatinum(II) molecular tweezer with a stimuli-responsive 2,2':6',2''-terpyridine spacer has been synthesized, which undergoes "U"- to "W"-shaped conformational transition upon adding Zn²⁺ ions. The molecular tweezer receptor displays a high binding affinity toward the complementary guests, with the implementation of Pt(II)···Pt(II) metal–metal interactions for the non-covalent tweezer systems. MMLCT absorbance simultaneously emerges in the visible-light region (470–620 nm), which can be sensitized by O₂ and thereby utilized for photo-catalyzed reactions in organic and aqueous media. Moreover, temporally "on-demand" photo-catalytic efficiency can be accomplished, *via* the successive addition of Zn(OTf)₂ and a competitive ligand to the supramolecular tweezer photosensitizers. Hence, the current study opens up new avenues toward intelligent photocatalytic materials *via* elaborate supramolecular engineering.

Received 14th September 2017,
Accepted 16th October 2017

DOI: 10.1039/c7qm00424a

rsc.li/frontiers-materials

CAS Key Laboratory of Soft Matter Chemistry, iChEM (Collaborative Innovation Center of Chemistry for Energy Materials), Department of Polymer Science and Engineering, University of Science and Technology of China, Hefei, Anhui 230026, P. R. China. E-mail: drfwang@ustc.edu.cn

† Electronic supplementary information (ESI) available: Synthesis, characterization, and other materials. See DOI: 10.1039/c7qm00424a



Feng Wang

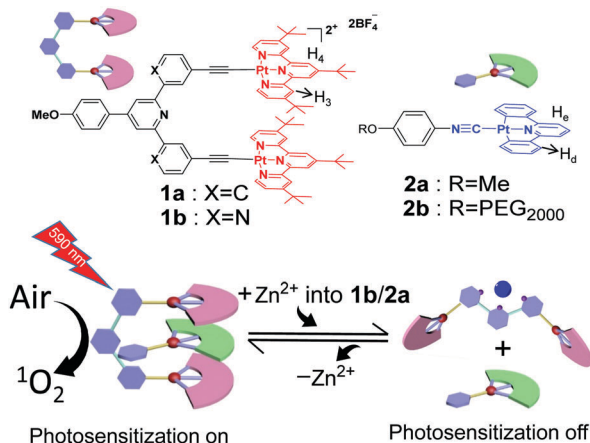
Feng Wang got his bachelor's degree from Hefei University of Technology in 2003. He then received his PhD in Chemistry from Zhejiang University under the supervision of Prof. Feihe Huang in 2009. He joined Prof. E. W. Meijer's group at Eindhoven University of Technology as a postdoctoral fellow. He joined the University of Science and Technology of China as an associate professor in 2011, and was promoted to full professor in

2016. His current research interests are focused on transition metal-based supramolecular assemblies for biomedical, optoelectronic, and catalytic applications.

Introduction

Visible-light photosensitization represents a sustainable method for organic transformation under mild conditions.^{1,2} Up to now, a variety of photosensitizers capable of undergoing energy transfer between their triplet excited states and oxygen molecules (O₂) have been developed, leading to the formation of reactive oxygen species for effective catalysis. However, the inherent photo-bleaching issues of the visible-light photosensitizers hamper their long-term use and storage with the threat of photo-degradation. In this regard, it is appealing to endow "on/off" functionality for the photosensitization process, which can significantly minimize the above-mentioned side effects.^{3–6} To attain this objective, organoplatinum(II)-based photosensitizers are regarded as one of the promising candidates.^{7–15} Owing to the square-planar geometry, they display a strong tendency to form intermolecular Pt(II)···Pt(II) interactions, accompanied by the presence of metal–metal-to-ligand charge transfer (MMLCT) optical signals in the visible-NIR region.^{16,17} By manipulating the distance and strength of Pt(II)···Pt(II) forces at the molecular level, the MMLCT spectroscopic signals can be elaborately modulated, which lays the basis for precise tempo-control over photo-sensitization/catalytic efficiencies.

Our research group is interested in constructing organoplatinum(II)-based molecular tweezers such as **1a** (Scheme 1) as the supramolecular receptor.^{18–27} It tends to encapsulate isocyanideplatinum(II) diphenylpyridine **2a** (Scheme 1) as the complementary guest, leading to the formation of intermolecular



Scheme 1 Schematic representation of the construction of supramolecular tweezer systems for “on/off”-switchable photosensitization.

Pt(II)··Pt(II) interactions for the non-covalent tweezer system. In the current study, we sought to incorporate dynamic switching elements into the molecular tweezer receptor, which triggers reversible guest encapsulation/release in response to external stimuli,^{28–32} and thereby regulates the emergence/disappearance of Pt(II)··Pt(II) MMLCT signals in a highly controllable manner.

Specifically, molecular tweezer **1b** (Scheme 1) has been designed and synthesized (Scheme S1 in the ESI[†]), in which 2,2':6',2''-terpyridine serves as the rigid spacer unit. As expected, **1b** prefers the “U”-shaped conformation (Fig. S1, ESI[†]),³³ with the adoption of co-facial conformation for two electron-deficient alkynylplatinum(II) terpyridine pincers. It is prone to sandwich neutral organoplatinum guest **2a** into its cavity. The presence of Pt(II)··Pt(II) interactions for the resulting tweezer complexes would lead to the generation of reactive oxygen species upon visible-light irradiation (Scheme 1), which can be further utilized for photo-catalyzed organic transformation. Upon addition of Zn(OTf)₂, **1b** is expected to undergo mechanical motion due to metal–ligand coordination between the Zn²⁺ ion and 2,2':6',2''-terpyridine spacer, resulting in the transition from “U”- to “W”-shaped conformation.^{34,35} Consequently, non-covalent tweezer structures are destroyed, leading to the vanishing of Pt(II)··Pt(II) interacting signals. Zn²⁺ ion-responsiveness for the supramolecular tweezer system provides a novel avenue toward intelligent photosensitization and photocatalytic materials.

Results and discussion

Spectroscopic measurements for molecular tweezer **1b** were first performed and compared with those of the counterpart molecular tweezer **1a**. For the dilute CHCl₃/CH₃CN (1:1, v/v) solution of **1b**, the maximum absorption and emission bands are located at 410 and 527 nm, respectively (Fig. 1a and b). According to the previous literatures, these bands are tentatively assigned to the admixture of dπ(Pt) → π*(*t*-Bu₃tpy) metal-to-ligand charge transfer (MLCT) and π(C≡CR) → π*(*t*-Bu₃tpy) ligand-to-ligand charge transfer (LLCT) bands.¹⁸ Notably, the MLCT/LLCT absorption and emission bands of **1b** are blue-shifted compared to

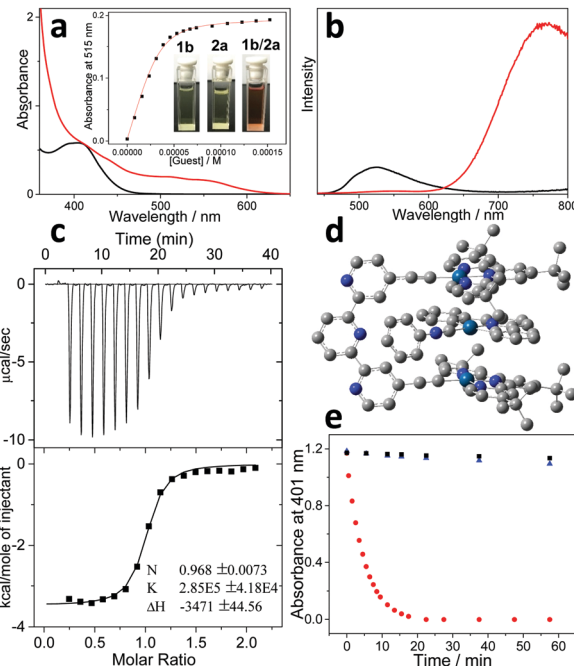


Fig. 1 (a) UV/Vis absorbance and (b) fluorescence changes upon addition of **2a** into **1b** (CHCl₃/CH₃CN = 1:1, 0.05 mM). Inset for (a): intensity changes at λ = 515 nm and the nonlinear curve fitting (red line). (c) ITC data for titrating **2a** (8.00 mM) into the solution (CHCl₃/CH₃CN = 1:1) of **1b** (0.40 mM). (d) Optimized structure of complex **1b/2a** via the DFT method. (e) Photosensitization (OLED lamp, 12 W, 590 nm) efficiency of **1b/2a** (●), **2a** (■), and **1b** (▲), by monitoring time-dependent absorbance of DMA at 401 nm.

those of **1a** (440 nm and 593 nm for the maximum absorption and emission bands, Fig. S2, ESI[†]).²⁴ Considering that **1a–b** feature the same platinum(II) center and *t*-Bu₃tpy main ligand, the relatively higher energy levels for MLCT/LLCT transition of **1a** can be ascribed to the structural variation on the ancillary dialkynyl ligand. Briefly, **1b** features a more electron-withdrawing ancillary ligand than that of **1a** (terpyridine *versus* diphenylpyridine), which renders the metal center more electron-deficient. As a result, it reduces the energy of the highest occupied molecular orbital (HOMO) for the platinum(II) center.³⁶

On this basis, non-covalent complexation was investigated between **1b** and the organoplatinum(II) guest **2a**. Upon adding an equimolar amount of **2a** (colorless) into **1b** (light yellow color), the mixed solution promptly becomes deep-red (Fig. 1a, inset). Simultaneously, a considerably bathochromically shifted band (λ_{max} = 515 nm) emerges in the UV-Vis spectrum (Fig. 1a). In addition, a new emission band appears in the near infrared region (λ_{max} = 780 nm), which shows enhanced intensity compared to the original MLCT/LLCT band (Fig. 1b). The newly formed bathochromically shifted signals can be assigned to the MMLCT (metal–metal-to-ligand charge transfer) transition,^{16,17} suggesting the proximity of the Pt(II) atoms upon complexation between **1b** and **2a**.

The binding thermodynamics for the resulting complex **1b/2a** can be further elucidated. Based on UV-Vis Job's plots, the MMLCT absorbance intensity reaches the maximum value

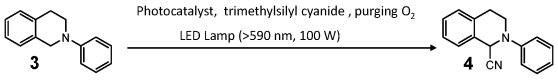
at the equivalent ratio, validating 1:1 binding stoichiometry between **1b** and **2a** (Fig. S4, ESI†). Nonlinear curve-fitting of the collected MMLCT absorbance data at 550 nm provides the K_a value of $(2.53 \pm 0.29) \times 10^5 \text{ M}^{-1}$ for complex **1b/2a** (Fig. 1a, inset). A similar binding affinity can be acquired *via* isothermal titration calorimetry (ITC) measurements ($K_a = (2.85 \pm 0.42) \times 10^5 \text{ M}^{-1}$) (Fig. 1c). It is worthy to note that complex **1b/2a** displays approximately five times enhancement for the binding strength compared to that of **1a/2a** ($K_{a,UV} = (4.69 \pm 0.13) \times 10^4 \text{ M}^{-1}$, Fig. S8, ESI†).

The exact binding mode for complex **1b/2a** was further clarified by density functional theory (DFT) calculation. As can be seen in Fig. 1d, the distances for the proximity Pt(II) atoms are determined to be 3.48 Å and 3.53 Å, with the Pt···Pt···Pt angle of 161.9°. Meanwhile, inter-planar π -distances between the electron-rich diphenylpyridine unit on **2a** and two electron-deficient terpyridine pincers on **1b** are calculated to be approximately 3.63 Å. The presence of electron donor-acceptor interactions between **1b** and **2a** is further validated by ^1H NMR measurements, which display remarkable upfield shifts for the aromatic protons on both **1b** and **2a** (−0.22, −0.30, −0.58 and −0.71 ppm for H_3 , H_4 , H_d , and H_e , respectively, Fig. S3, ESI†). Accordingly, it can be concluded that non-covalent complexation between **1b** and **2a** is co-driven by Pt(II)···Pt(II) metal-metal and electron donor-acceptor interactions.

In view of the fact that complex **1b/2a** features bathochromically shifted MMLCT absorbance, its visible-light photosensitization capability was then investigated. When photo-exciting the mixture of **1b/2a** and 9,10-dimethylantracene (DMA) with an OLED lamp (12 w, 590 nm), the absorbance of DMA at 401 nm decays and levels off after 20 min (Fig. 1e). Hence, it validates the generation of singlet oxygen ($^1\text{O}_2$) *in situ*, which is captured by DMA to form 9,10-dimethylantracene-9,10-endoperoxide. In sharp contrast, DMA absorbance hardly shows any changes for the individual species (**1b** or **2a**) (Fig. 1e), because of the absence of MMLCT transition signals. In addition, photosensitization capability can be influenced by the non-covalent complexation strength, as evidenced by the higher $^1\text{O}_2$ generation efficiency of complex **1b/2a** than that of **1a/2a** ($725 \text{ min}^{-1} \text{ M}^{-1}$ vs. $322 \text{ min}^{-1} \text{ M}^{-1}$, Fig. S11, ESI†).³⁷

Furthermore, the photo-catalytic efficiency of complex **1b/2a** was examined, by performing the oxidative cyanation reaction for *N*-phenyl-1,2,3,4-tetrahydroisoquinoline **3** (Table 1). In detail, upon irradiating (LED lamp, > 590 nm, 100 W) the reactants and **1b/2a** (1.0–0.2 mol%), 89–94% product yields can be achieved (entries 1–3 in Table 1). In stark contrast, almost no conversion can be detected for the individual species even with prolonged irradiation time (either **1b** or **2a**, entries 7–8 in Table 1). Besides, the turnover (TON) value of **1b/2a** is 1.37 times higher than that of **1a/2a** (entries 1 and 4 in Table 1), which is consistent with the stronger $^1\text{O}_2$ generation capability of the former complex. The photocatalytic mechanism can be explained as follows: due to the spectral overlap between photo-irradiation wavelength and the MMLCT absorbance of **1b/2a**, $^1\text{O}_2$ can be generated *in situ*. The reactive oxygen species interacts with **3** to afford the unstable iminium ion intermediate,³⁸ which further reacts with trimethylsilyl cyanide (TMSCN) to give the cyanation product **4**.

Table 1 Photo-oxidative cyanation of **3** to **4**^a

					
Entry	Photocatalyst	Time [h]	Conversion [%]	Yield [%]	TON [h ^{−1}]
1	1b/2a	1.25	100	92	184.0
2 ^b	1b/2a	0.42	100	94	223.8
3 ^c	1b/2a	4	98	89	111.3
4 ^d	1a/2a	1.67	100	90	134.7
5 ^e	1b/2a	24	4	n.d.	—
6 ^f	1b/2a	24	2	n.d.	—
7 ^g	1b	24	7	n.d.	—
8 ^h	2a	24	4	n.d.	—

^a Compound **3** (10.00 mmol L^{−1}), photocatalyst (0.4 mol%), and TMSCN (15.00 mmol L^{−1}) are dissolved in CHCl₃:CH₃CN (1:1, 10 mL), with O₂ bubbling for 10 seconds. After the photo-catalyzed reaction, the solvent was evaporated and the residue was subjected to ^1H NMR analysis. Conversion was determined by crude ^1H NMR analysis using 4,4'-dimethyl-2,2'-bipyridine as the internal standard. Yield was calculated based on the starting amount of substrate. The similar reaction conditions described in entry a were also used for entries b–h, except where otherwise specified. ^b Catalyst loading was 1 mol%. ^c Catalyst loading was 0.2 mol%. ^d Complex **1a/2a** was employed as the catalyst. ^e N₂ instead of O₂ was purged into the solution for 30 seconds. ^f The solution mixture was kept in the dark. ^g **1b** was employed as the catalyst. ^h **2a** was employed as the catalyst. n.d. = not determined.

No conversion can be detected with the absence of oxygen or light (entries 5 and 6 in Table 1), validating that $^1\text{O}_2$ is the active oxidant during the organic transformation process.

Considering that water is a green and environmentally friendly medium, it is keenly pursued to perform photocatalytic organic transformation in an aqueous solution. To guarantee sufficient water-solubility of the supramolecular photocatalyst, poly(ethylene glycol) (PEG2000) was attached to the guest structure (guest **2b**, see Scheme 1). For the resulting complex **1b/2b**, color change together with the appearance of MMLCT transition signals takes place in water (Fig. 2b), which

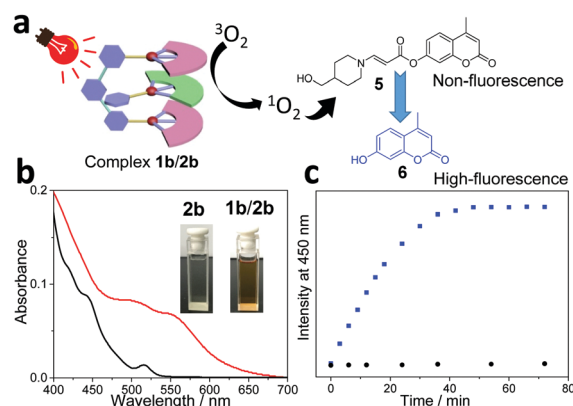


Fig. 2 (a) Schematic representation for the photo-cleavage of coumarin derivative **5** with complex **1b/2b** as the catalyst. (b) UV/Vis absorbance of **2b** and complex **1b/2b** (0.05 mM, 95% water/5% DMF). Inset: The solution colors of **2b** and **1b/2b**. (c) Time-dependent fluorescence changes of **5** (20 μM in 95% water/5% DMF) upon visible-light irradiation (OLED lamp, 12 w, 590 nm), with the employment of **1b/2b** (■) and **1b/2a** (●) as the photocatalysts.

are similar to those of complex **1b/2a** in an organic medium. Notably, the presence of a PEG chain exerts minor impact on the non-covalent binding affinity, since both complexes **1b/2a** and **1b/2b** show comparable K_a values ($K_{a,UV} = (2.30 \pm 0.22) \times 10^5 \text{ M}^{-1}$ and $K_{a,ITC} = (3.90 \pm 0.17) \times 10^5 \text{ M}^{-1}$ for **1b/2b** in $\text{CHCl}_3:\text{CH}_3\text{CN}$ (1:1, v/v), Fig. S6 and S7, ESI†). On this basis, photo-triggered cleavage of coumarin derivative **5** in an aqueous solution was performed, by employing **1b/2b** as the catalyst (Fig. 2a). As previously reported by You and others,^{39,40} the fluorescence of **5** is significantly quenched due to the presence of the amino-acrylate linker. Upon photo-irradiation (590 nm, 12 w), the linker can be cleaved by $^1\text{O}_2$, leading to the formation of highly fluorescent product **6**. In the current system, the emission signal at 450 nm gradually increases and reaches a plateau after 40 min (Fig. 2c). ^1H NMR experiments provide additional evidence for the quantitative conversion of **5** to **6**, which shows upfield shifting of the aromatic protons after the photo-cleavage process (Fig. S13, ESI†). Under the same conditions, no emission intensity varies for complex **1b/2a** (Fig. 2c). Hence, attachment of a PEG solubilizing group on the supramolecular tweezer structure represents an efficient approach for photo-catalytic reactions in aqueous solution.

Stimuli-responsiveness of the non-covalent tweezer complexes toward Zn^{2+} ions was then exploited. As an initial step, we exploited cation-triggered nanomechanical motion of **1b**. Upon gradually titrating $\text{Zn}(\text{OTf})_2$ into the $\text{CHCl}_3:\text{CH}_3\text{CN}$ (1:1, v/v) solution of **1b**, the MLCT/LLCT absorbance located at 410 nm exhibits a hypsochromic shift, accompanied by an isosbestic point at 427 nm (Fig. S15, ESI†). Blue-shifting of the MLCT/LLCT band primarily arises from the decreased electron-donating capability of the ancillary ligand, denoting metal-ligand complexation between Zn^{2+} ions and the rigid terpyridine spacer on **1b**. Simultaneously, “U”- to “W”-shaped conformational transition takes place for **1b**, which further affects the non-covalent binding affinity toward the complementary guest **2a**. It can be directly reflected by the disappearance of MMLCT absorbance and emission bands (Fig. 3a and Fig. S16, ESI†). Further evidence for the decomplexation between **1b** and **2a** came from ITC experiments, as evidenced by the negligible heat exchange upon titrating **2a** into the mixture solution of **1b/Zn(OTf)₂** (Fig. S17a, ESI†). In sharp contrast, the presence of

Zn^{2+} ions hardly influences the isothermal curve between **1a** and **2a** (Fig. S17b, ESI†), validating the importance of dynamic switching elements for cation-responsive molecular tweezer/guest complexation behaviors.

Notably, the reversible “on/off” switching of the $\text{Pt(II)} \cdots \text{Pt(II)}$ absorbance signal for **1b/2a** (Fig. 3a) provides extra control over their photo-catalytic efficiency, which can be demonstrated by monitoring the conversion from **3** to **4** upon addition/removal of $\text{Zn}(\text{OTf})_2$. In detail, when the Zn^{2+} ion is added to complex **1b/2a**, it breaks up the photo-catalytic capability (Fig. S18, ESI†). The successive addition of unsubstituted terpyridine as the competitive ligand⁴¹ traps Zn^{2+} ions, and thereby leads to the recovery of photo-catalytic efficiency (Fig. S18, ESI†). Noteworthy, with the sequential addition of $\text{Zn}(\text{OTf})_2$ and unsubstituted terpyridine, “on-demand” revival and loss of photo-oxidation capability for **3** can be achieved for several repeated cycles (Fig. 3b).

Conclusions

In summary, herein we have successfully developed a novel supramolecular tweezer system with the involvement of $\text{Pt(II)} \cdots \text{Pt(II)}$ metal-metal interactions. For the non-covalent molecular tweezer/guest complexes **1b/2a** and **1b/2b**, MMLCT absorbance signals emerge in the visible-light region, which can be sensitized by O_2 . As a result, they can be utilized for photo-oxidative cyanation and photo-cleavage reactions in organic and aqueous media. More importantly, temporally “on-demand” photo-catalytic efficiency can be achieved, by taking advantage of the Zn^{2+} -responsive conformational switch of the molecular tweezer receptor. Hence, the current study opens up new avenues toward intelligent photocatalytic materials *via* elaborate supramolecular design.

Conflicts of interest

There are no conflicts to declare.

Acknowledgements

This work was supported by the National Natural Science Foundation of China (21274139), the Fundamental Research Funds for the Central Universities (WK3450000001), and CAS Youth Innovation Promotion Association (2015365).

Notes and references

- 1 T. P. Yoon, M. A. Ischay and J. Du, *Nat. Chem.*, 2010, **2**, 527.
- 2 C. K. Prier, D. A. Rankic and D. W. MacMillan, *Chem. Rev.*, 2013, **113**, 5322.
- 3 K. Liu, Y. Liu, Y. Yao, H. Yuan, S. Wang, Z. Wang and X. Zhang, *Angew. Chem., Int. Ed.*, 2013, **52**, 8285.
- 4 L.-L. Hou, X.-Y. Zhang, T. C. Pijper, W. R. Browne and B. L. Feringa, *J. Am. Chem. Soc.*, 2014, **136**, 910.
- 5 Y. Jiao, K. Liu, G. Wang, Y. Wang and X. Zhang, *Chem. Sci.*, 2015, **6**, 3975.

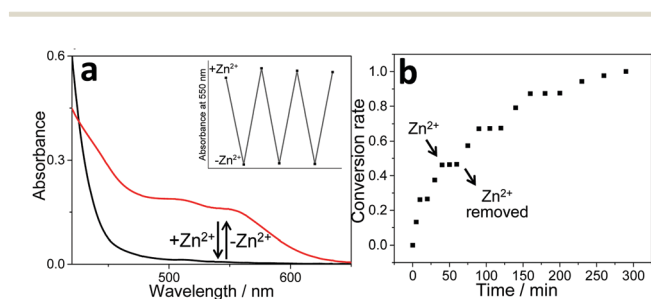


Fig. 3 (a) UV-Vis spectral changes of complex **1b/2a** in $\text{CHCl}_3/\text{CH}_3\text{CN}$ (1:1, v/v) upon sequential addition of $\text{Zn}(\text{OTf})_2$ and cyclen as the competitive ligand to trap Zn^{2+} ions. The inset shows the changes in the absorption intensity at 550 nm. (b) Photocatalytic conversion of **3** to **4** upon sequential addition of $\text{Zn}(\text{OTf})_2$ and unsubstituted terpyridine (as the competitive ligand to trap Zn^{2+} ion)⁴¹ to the photo-catalyst **1b/2a** in $\text{CHCl}_3/\text{CH}_3\text{CN}$ (1:1, v/v).

- 6 X.-Q. Wang, Q. Lei, J.-Y. Zhu, W.-J. Wang, Q. Cheng, F. Gao, Y.-X. Sun and X.-Z. Zhang, *ACS Appl. Mater. Interfaces*, 2016, **8**, 22892.
- 7 K. Feng, R.-Y. Zhang, L.-Z. Wu, B. Tu, M.-L. Peng, L.-P. Zhang, D. Zhao and C.-H. Tung, *J. Am. Chem. Soc.*, 2006, **128**, 14685.
- 8 J.-J. Zhong, Q.-Y. Meng, G.-X. Wang, Q. Liu, B. Chen, K. Feng, C.-H. Tung and L.-Z. Wu, *Chem. – Eur. J.*, 2013, **19**, 6443.
- 9 Q.-Y. Meng, T. Lei, L.-M. Zhao, C.-J. Wu, J.-J. Zhong, X.-W. Gao, C.-H. Tung and L.-Z. Wu, *Org. Lett.*, 2014, **16**, 5968.
- 10 P.-K. Chow, G. Cheng, G. S. M. Tong, W.-P. To, W.-L. Kwong, K.-H. Low, C.-C. Kwok, C. Ma and C.-M. Che, *Angew. Chem., Int. Ed.*, 2015, **127**, 2112.
- 11 J.-J. Zhong, C. Yang, X.-Y. Chang, C. Zou, W. Lu and C.-M. Che, *Chem. Commun.*, 2017, **53**, 8948.
- 12 K. Mori, K. Watanabe, M. Kawashima, M. Che and H. Yamashita, *J. Phys. Chem. C*, 2011, **115**, 1044.
- 13 K. Mori, K. Watanabe, K. Fuku and H. Yamashita, *Chem. – Eur. J.*, 2012, **18**, 415.
- 14 K. Mori, K. Watanabe, Y. Terai, Y. Fujiwara and H. Yamashita, *Chem. – Eur. J.*, 2012, **18**, 11371.
- 15 K. Mori and H. Yamashita, *Chem. – Eur. J.*, 2016, **22**, 11122.
- 16 K. M.-C. Wong and V. W.-W. Yam, *Acc. Chem. Res.*, 2011, **44**, 424.
- 17 S. Y.-L. Leung, A. Y.-Y. Tam, C.-H. Tao, H. S. Chow and V. W.-W. Yam, *J. Am. Chem. Soc.*, 2012, **134**, 1047.
- 18 Y. Tanaka, K. M.-C. Wong and V. W.-W. Yam, *Chem. Sci.*, 2012, **3**, 1185.
- 19 Y. Tanaka, K. M.-C. Wong and V. W.-W. Yam, *Chem. – Eur. J.*, 2013, **19**, 390.
- 20 Y. Tanaka, K. M.-C. Wong and V. W.-W. Yam, *Angew. Chem., Int. Ed.*, 2013, **125**, 14367.
- 21 A. K. W. Chan, W. H. Lam, Y. Tanaka, K. M. C. Wong and V. W. W. Yam, *Proc. Natl. Acad. Sci. U. S. A.*, 2015, **112**, 690.
- 22 T. Haino, T. Fujii, A. Watanabe and U. Takayanagi, *Proc. Natl. Acad. Sci. U. S. A.*, 2009, **106**, 10477.
- 23 Y.-J. He, T.-H. Tu, M.-K. Su, C.-W. Yang, K. V. Kong and Y.-T. Chan, *J. Am. Chem. Soc.*, 2017, **139**, 4218.
- 24 Y.-K. Tian, Y.-G. Shi, Z.-S. Yang and F. Wang, *Angew. Chem., Int. Ed.*, 2014, **53**, 6090.
- 25 Z. Gao, Y.-F. Han, J.-J. Chen, X. Wang and F. Wang, *Chem. – Asian J.*, 2016, **11**, 1775.
- 26 Z.-J. Li, Y.-F. Han, F. Jin, Z.-C. Gao, Z. Gao, L. Ao and F. Wang, *Dalton Trans.*, 2016, **45**, 17290.
- 27 Z.-J. Li, Y.-F. Han, Z.-C. Gao and F. Wang, *ACS Catal.*, 2017, **7**, 4676.
- 28 X. Yan, T. R. Cook, P. Wang, F. Huang and P. J. Stang, *Nat. Chem.*, 2015, **7**, 342.
- 29 M. Zhang, M. L. Saha, M. Wang, Z. Zhou, B. Song, C. Lu, X. Yan, X. Li, F. Huang, S. Yin and P. J. Stang, *J. Am. Chem. Soc.*, 2015, **139**, 5067.
- 30 X. Yan, M. Wang, T. R. Cook, M. Zhang, M. L. Saha, Z. Zhou, X. Li, F. Huang and P. J. Stang, *J. Am. Chem. Soc.*, 2016, **138**, 4580.
- 31 S. Chen, L.-J. Chen, H.-B. Yang, H. Tian and W. Zhu, *J. Am. Chem. Soc.*, 2012, **134**, 13596.
- 32 B. Jiang, J. Zhang, J.-Q. Ma, W. Zheng, L.-J. Chen, B. Sun, C. Li, B.-W. Hu, H. Tan., X. Li and H.-B. Yang, *J. Am. Chem. Soc.*, 2016, **138**, 738.
- 33 B. Doistau, A. Tron, S. A. Denisov, G. Jonusauskas, N. D. McClenaghan, G. Gontard, V. Marvaud, B. Hasenknopf and G. Vives, *Chem. – Eur. J.*, 2014, **20**, 15799.
- 34 A. Petitjean, R. G. Khoury, N. Kyritsakas and J.-M. Lehn, *J. Am. Chem. Soc.*, 2004, **126**, 6637.
- 35 B. Doistau, L. Benda, J.-L. Cantin, L.-M. Chamoiseau, E. Ruiz, V. Marvaud, B. Hasenknopf and G. Vives, *J. Am. Chem. Soc.*, 2017, **139**, 9213.
- 36 F. Guo, W. Sun, Y. Liu and K. Schanze, *Inorg. Chem.*, 2005, **44**, 4055.
- 37 Y. Liu and J. Zhang, *Chem. Commun.*, 2012, **48**, 3751.
- 38 W.-P. Wong, G. S.-M. Tong, W. Lu, C. Ma, J. Liu, A. L.-F. Chow and C.-M. Che, *Angew. Chem., Int. Ed.*, 2012, **51**, 2654.
- 39 A. M. L. Hossion, M. Bio, G. Nkepang, S. G. Awuah and Y. You, *ACS Med. Chem. Lett.*, 2013, **4**, 124.
- 40 Y. Liu, T. Pauloeherl, S. I. Presolski, L. Albertazzi, A. R. A. Palmans and E. W. Meijer, *J. Am. Chem. Soc.*, 2015, **137**, 13096.
- 41 For the temporally “on-demand” photo-catalytic experiments, we initially employed cyclen to trap Zn²⁺ ions. However, the amine units on cyclen might influence the photosensitization efficiency of complex **1b/2a**, leading to the irreversible deactivation of the photo-catalytic efficiency. To avoid this issue, unsubstituted terpyridine was chosen as the competitive ligand instead of cyclen.